Diffractive generalized phase contrast for adaptive phase imaging and optical security

Palima, Darwin; Glückstad, Jesper

Published in:
Optics Express

Link to article, DOI:
10.1364/OE.20.001370

Publication date:
2012

Document Version
Publisher's PDF, also known as Version of record

Diffractive generalized phase contrast for adaptive phase imaging and optical security

Darwin Palima and Jesper Glückstad*

DTU Fotonik, Department of Photonics Engineering, Technical University of Denmark, DK-2800 Kgs. Lyngby, Denmark

*jesper.gluckstad@fotonik.dtu.dk

www.ppo.dk

Abstract: We analyze the properties of Generalized Phase Contrast (GPC) when the input phase modulation is implemented using diffractive gratings. In GPC applications for patterned illumination, the use of a dynamic diffractive optical element for encoding the GPC input phase allows for on-the-fly optimization of the input aperture parameters according to desired output characteristics. For wavefront sensing, the achieved aperture control opens a new degree of freedom for improving the accuracy of quantitative phase imaging. Diffractive GPC input modulation also fits well with grating-based optical security applications and can be used to create phase-based information channels for enhanced information security.

OCIS codes: (110.0110) Imaging systems; (120.0120) Instrumentation, measurement, and metrology; (100.0100) Image processing; (090.1970) Diffractive optics.

References and Links

1. G. Whyte and J. Courtial, "Experimental demonstration of holographic three-dimensional light shaping using a Gerchberg–Saxton algorithm," New J. Phys. **7**, 117–117 (2005).
2. T. Ando, Y. Ohtake, N. Matsumoto, T. Inoue, and N. Fukuchi, "Mode purities of Laguerre-Gaussian beams generated via complex-amplitude modulation using phase-only spatial light modulators," Opt. Lett. **34**(1), 34–36 (2009).
3. V. Arrizón, U. Ruiz, G. Mendez, and A. Apolinar-Iribe, "Zero order synthetic hologram with a sinusoidal phase carrier for generation of multiple beams," Opt. Express **17**(4), 2663–2669 (2009).
4. J. A. Davis, J. Guertin, and D. M. Cottrell, "Diffraction-free beams generated with programmable spatial light modulators," Appl. Opt. **32**(31), 6368–6370 (1993).
5. V. Arrizón, D. Sánchez-de-la-Llave, U. Ruiz, and G. Méndez, "Efficient generation of an arbitrary nondiffracting Bessel beam employing its phase modulation," Opt. Lett. **34**(9), 1456–1458 (2009).
6. M. Antkowiak, M. L. Torres-Mapa, F. Gunn-Moore, and K. Dholakia, "Application of dynamic diffractive optics for enhanced femtosecond laser based cell transfection," J Biophoton. **3**(10-11), 696–705 (2010).
7. Y. Hayasaki, T. Sugimoto, A. Takita, and N. Nishida, "Variable holographic femtosecond laser processing by use of a spatial light modulator," Appl. Phys. Lett. **87**(3), 031101 (2005).
8. E. Papagiakoumou, F. Anselmi, A. Bègue, V. de Sars, J. Glückstad, E. Y. Isacoff, and V. Emiliani, "Scanless two-photon excitation of channelrhodopsin-2," Nat. Methods **7**(10), 848–854 (2010).
9. J. Liesener, M. Reicherter, T. Haist, and H. Tiziani, "Multi-functional optical tweezers using computer-generated holograms," Opt. Commun. **185**(1-3), 77–82 (2000).
10. D. G. Grier, "A revolution in optical manipulation," Nature **424**(6950), 810–816 (2003).
11. J. P. Kirk and A. L. Jones, "Phase-Only Complex-Valued Spatial Filter," J. Opt. Soc. Am. **61**(8), 1023–1028 (1971).
12. J. A. Davis, D. M. Cottrell, J. Campos, M. J. Yzuel, and I. Moreno, "Encoding Amplitude Information onto Phase-Only Filters," Appl. Opt. **38**(23), 5004–5013 (1999).
13. H. Goto, T. Konishi, and K. Itoh, "Simultaneous amplitude and phase modulation by a discrete phase-only filter," Opt. Lett. **34**(5), 641–643 (2009).
14. C. Maurer, A. Jesacher, S. Bernet, and M. Ritsch-Marte, "What spatial light modulators can do for optical microscopy," Laser Photon. Rev. **5**(1), 81–101 (2011).
15. G. Mínguez-Vega, V. R. Supradeepa, O. Mendoza-Yero, and A. M. Weiner, "Reconfigurable all-diffractive optical filters using phase-only spatial light modulators," Opt. Lett. **35**(14), 2406–2408 (2010).
16. J. Glückstad and D. Palima, *Generalized Phase Contrast: Applications in Optics and Photonics* (Springer, 2009)
17. D. Palima and J. Glückstad, "Comparison of generalized phase contrast and computer generated holography for laser image projection," Opt. Express **16**(8), 5338–5349 (2008).
18. Y.-Y. Cheng and J. C. Wyant, "Phase shifter calibration in phase-shifting interferometry," Appl. Opt. **24**(18), 3049 (1985).

#151449 - $15.00 USD Received 21 Jul 2011; revised 14 Sep 2011; accepted 3 Oct 2011; published 9 Jan 2012

19. P. J. Rodrigo, D. Palima, and J. Glückstad, "Accurate quantitative phase imaging using generalized phase contrast," Opt. Express **16**(4), 2740–2751 (2008).
20. P. C. Mogensen and J. Glückstad, "Phase-only optical encryption," Opt. Lett. **25**(8), 566–568 (2000).

1. Introduction

The advent of commercially available spatial light modulators (SLM) witnessed a renewed interest in various approaches for dynamic and reconfigurable lightshaping applications. SLMs can synthesize assorted beams [1–3], including non-diffracting beams [4,5], for applications such as material processing [6,7], photoexcitation [8], and micro-manipulation [9,10]. SLM-based filters have applications in optical processing [11–13], microscopy [14] and pulseshaping [15]. SLMs are typically used as computer-generated holograms (CGHs) that can perturb incident light to create user-designed diffraction fields. Unlike conventional holograms that diffract light to mimic the complex field scattered from a prerecorded object, CGHs are numerically designed by solving an inverse diffraction problem and omits the recording process.

SLMs are also used as input phase modulators in various applications of Generalized Phase Contrast (GPC) [16], a technique that extends conventional phase contrast to operate beyond the weak phase limit. The GPC technique can have certain advantages over computer-generated holography [17]. For example, synthesizing structured illumination with GPC simply requires input phase patterns that mimic the desired illumination structures. The spatial phase modulation patterns are converted into high-contrast intensity distributions at the output of a GPC system. The minimal computational overhead in designing the GPC phase masks liberates computing power for other needed performance enhancements. However, CGH and diffractive optics can be invaluable when generating light fields aiming with controlled amplitude and phase.

In this work, we explore a new approach that combines the GPC technique with a diffractively modulated input. Here the input contains not only the conventional input phase, but also a diffractive element. Conventional GPC uses low spatial frequency components to synthesize a phase-shifted reference beam (i.e., synthetic reference wave, SRW). The interference of the SRW with the input phase image at the output plane creates high-contrast intensity distributions. In the present work, higher-order diffraction is utilized to synthesize the reference wave. We will describe the formalism in the next section and subsequently show, in the following sections, how this approach can enable dynamic input optimization in various applications, including patterned light synthesis, quantitative phase imaging, and optical cryptography.

2. Diffractive phase modulation in generalized phase contrast

The conventional GPC input field is

$$p_C(x,y) = a(x,y)\exp\left[\mathrm{i}\phi(x,y)\right], \tag{1}$$

where the amplitude modulation, $a(x,y)$, (e.g. an aperture function or Gaussian illumination) is coupled with a phase modulation, $\phi(x,y)$. The image of this input interferes with the synthesized reference wave at the output plane to form an intensity pattern,

$$I(x',y') \approx \left| a(x',y')\exp\left[\mathrm{i}\phi(x',y')\right] + r_S(x',y') \right|^2, \tag{2}$$

where the reference wave is a slowly varying function,

$$r_S(x,y) = \bar{\alpha}\left[\exp(\mathrm{i}\theta) - 1\right]\Im^{-1}\left\{S(f_x,f_y)\,\Im\left\{a(x,y)\right\}\right\}. \tag{3}$$

This expression incorporates the effect of the input phase into a complex amplitude factor,

$$\bar{\alpha} = \iint a(x,y)\exp\left[\mathrm{i}\phi(x,y)\right]dxdy \Big/ \iint a(x,y)\,dxdy, \tag{4}$$

#151449 - $15.00 USD Received 21 Jul 2011; revised 14 Sep 2011; accepted 3 Oct 2011; published 9 Jan 2012

which represents the normalized zero-order term of the input's Fourier transform.

The present GPC approach uses diffractive input modulation and is schematically depicted in Fig. 1. This differs from the conventional setup in that the input phase modulation is now combined with a phase-only diffractive optical element, such as a blazed grating or carrier frequency modulation, for example. Under standard conditions, the GPC output will visualize this input phase, including the additional diffractive phase modulations. To render only the phase input, we must reconfigure the optical setup to match the diffractive phase modulation, as we will describe shortly.

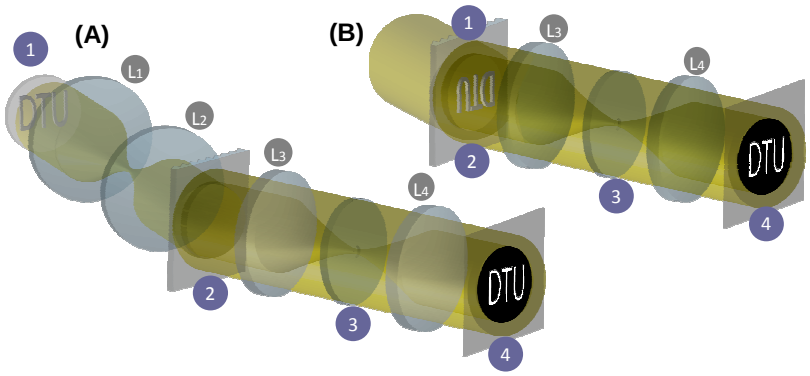

Fig. 1. Schematic of GPC with diffractive input modulation (A) Dual modulation system where the phase object, 1, is relayed to a diffractive GPC input, 2, using lenses L_1/L_2 (B) Single modulation system where the GPC input plane contains both the phase object, 1, and the diffracting element, 2. In both systems, the resulting phase modulation along a diffraction order is imaged at the output plane, 4, and transformed into a high-contrast intensity pattern via interference with a common-path reference wave synthesized by the phase contrast filter, 3.

In the present approach, we incorporate an additional diffractive phase modulation to the input, which could be done in standalone configuration (Fig. 1a) or by field multiplication of a relayed phase modulation to a diffracting plane (Fig. 1b). The modified input becomes

$$\begin{aligned} p_M(x,y) &= a(x,y)\exp\left[\mathrm{i}\phi(x,y)\right]\exp\left[\mathrm{i}\phi_D(x,y)\right] \\ &= a(x,y)\exp\left\{\mathrm{i}\left[\phi(x,y)+\phi_D(x,y)\right]\right\}\ , \end{aligned} \tag{5}$$

where $\phi_D(x,y)$ is the phase-only diffractive modulation. In standard GPC, this will simply cause the system to visualize the modified phase input, $\phi(x,y)+\phi_D(x,y)$, instead of the original $\phi(x,y)$. By proper choice of the diffractive element and a corresponding adjustment of the optical system, it is possible to render an output intensity pattern that is based only on the phase $\phi(x,y)$.

As a simple starting point, let's consider a blazed grating as our additional phase-only diffractive element. The input in this case becomes

$$p_M(x,y) = p_C(x,y)\left\{\left[\exp\left(2\pi\mathrm{i}f_0x\right)\mathrm{rect}\left(x/2w\right)\right]\otimes\mathrm{comb}\left(x/X\right)\right\}, \tag{6}$$

where w is the width of each repeated segment of the grating; X is the grating period; f_0 is a constant related to the blaze angle; $\mathrm{rect}(x)=1$ for $|x|\le\frac{1}{2}$ and zero otherwise; and $\mathrm{comb}(x)=\sum_{-\infty}^{\infty}\delta(x-n)$. The field at the filter is directly proportional to Fourier transform

$$P_M(f_x,f_y) = P_C(f_x,f_y)\otimes\left\{2wX\,\mathrm{sinc}\left[2w\left(f_x-f_0\right)\right]\mathrm{comb}\left(Xf_x\right)\right\}. \tag{7}$$

In the ideal case of a 100% fill factor (i.e., $X = 2w$) and a blaze angle f_0 = m/X, the comb aligns with the zeros of the sinc function except at the m^{th}-order where all of the energy goes:

#151449 - $15.00 USD Received 21 Jul 2011; revised 14 Sep 2011; accepted 3 Oct 2011; published 9 Jan 2012

$$P_M(f_x, f_y) = P_C(f_x - \mathrm{m}/X, f_y)2wX \sin c\left(\mathrm{m}/X - f_0\right). \quad (8)$$

Aligning the GPC axis along this diffraction order will cancel the frequency offset to reproduce the usual intensity pattern at the GPC output. For non-ideal blaze angles, the sinc term in Eq. (7) is less than 1 and light will be lost into spurious diffraction orders. However, this enables us to control the input amplitude by spatially modulating the blaze angle, which may be exploited to optimize desired output metrics. We will consider various examples in the following sections to illustrate this.

3. Dynamic input aperture optimization for patterned illumination

One direct use of the diffractive modulation is to implement dynamically controlled input apertures. It is well-established in GPC literature that output optimization requires a proper match between the input and filter parameters. When using circular input apertures, for example, the optimal size of the phase shifting region in the GPC filter is specified relative to the Airy disc radius. However, it is more practical to use high quality static filters and instead adjust the Airy disc radius using the input aperture. One way to implement diffractive apertures is to encode high frequency carrier beyond the desired clear region to scatter light outside the finite apertures of the optical system. This approach essentially combines diffractive encoding with spatial filtering. Alternately, the designated clear aperture may be encoded onto a carrier and the GPC optics aligned along this carrier.

To evaluate the performance of GPC when using phase inputs on a carrier, we used a phase-only SLM (Holoeye HOE 1080) to encode both the input phase and the diffracting element (see Fig. 1B). Although blazed carriers can optimize efficiency, we used binary carrier gratings in proof-of-concept experiments due to device resolution limits. Binary gratings were phase-encoded onto circular regions within an otherwise uniform phase background on the SLM. The programmed phase modulation is read out using an expanded beam from an Nd:YVO_4 laser (Laser Quantum Excel, λ = 532 nm). Using an off-axis readout beam diffracts the 1st-order beam perpendicular to the SLM, which is aligned along the optical axis of the GPC system that uses a π-shifting circular filter. Typical output patterns are shown in Fig. 2.

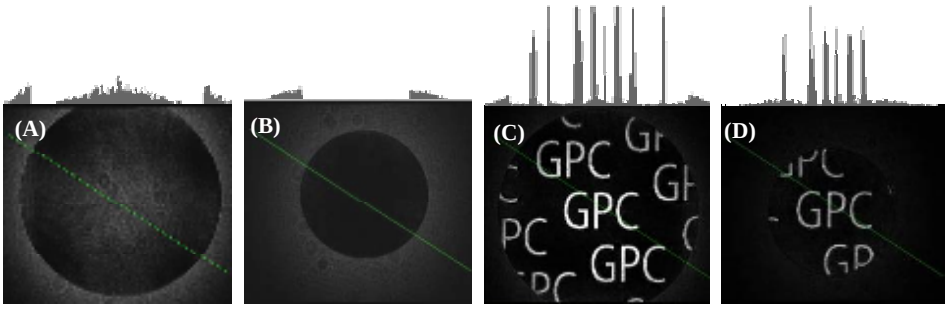

Fig. 2. Intensity patterns generated using GPC with diffractive/modulated inputs. (A) The central bump indicates that the aperture size results in an out-of-phase SRW that is twice as strong as the aperture illumination on-axis. (B) The dark background circular aperture the aperture size results in an SRW that cancels the aperture illumination on-axis. (C) Circular aperture from (A) with added phase modulation; (C) Circular aperture from (A) with added phase modulation. Intensity linescans (green line) are shown above the respective images.

Using the setup in Fig. 1B, we used the SLM to create a diffractive phase input, which corresponds to the multiplication of the phase object with a high frequency grating defined on a circular region with the aim of diffracting exactly the light coming from the circular region to the entrance pupil. Figures 2(a) and 2(b) show the GPC output when there is no phase object and we only encode circular carrier gratings with different radii; Figs. 2(c) and 2(d) show the output when a phase object is multiplied to the gratings. These results reproduce previous on-axis GPC calibration based on mechanical input apertures. This time, the

#151449 - $15.00 USD Received 21 Jul 2011; revised 14 Sep 2011; accepted 3 Oct 2011; published 9 Jan 2012

diffractive input enables us to vary the radius of the circular grating region to create a GPC system with a software-optimizable nonmechanical aperture.

The output presented in Figs. 2(a) and (b) correspond to a GPC system with a uniform phase input within a circular aperture. The interference pattern at the GPC output in this case is described by rewriting Eq. (2)

$$I(x',y') \approx \left| \mathrm{circ}\left(\sqrt{x'^2+y'^2}/\Delta R\right) \exp\left[\mathrm{i}\phi_0\right] + r_S(x',y') \right|^2 . \tag{9}$$

The circular input and filter apertures create a circularly symmetric synthesized reference wave, $r_S(r') = -4\pi\Delta R \int_0^{\Delta f_R} J_1(2\pi\Delta R f_r) J_1(2\pi r' f_r)\,\mathrm{d}f_r$, where the Fourier transforms in Eq. (3) are now replaced with the zero-order Hankel transform and we applied $\bar{\alpha}=1$ and $\theta=\pi$. Adjusting the circular grating radius, ΔR, allows us to control the synthesized reference wave, e.g. to achieve darkness within the image of the circular region, as seen in Fig. 2(b), or to create an intensity bump at the center, as in Fig. 2(a). This control over the reference wave is important when additional phase patterns are included on the gratings. Although Figs. 2(c) and (d) both show that added phase patterns are visualized as high-contrast images without the attending high-frequency carrier, the input aperture size affects the intensity and contrast of the generated patterns. The results show that the GPC output pattern in Fig. 2(c), which was obtained by incorporating the phase pattern onto the circular grating in Fig. 2(a), is more intense than the pattern in Fig. (d), which used the circular grating in Fig. 2(b). These results are consistent with earlier results based on carrier-free phase inputs with mechanical truncating apertures.

4. Dynamic input optimization for SLM-assisted adaptive phase imaging

The dual modulation setup in Fig. 1(A) can be used for imaging external phase objects. Here, an image of the phase object is first relayed onto the diffracting element at the GPC input plane, which then creates a high-contrast image of the diffracted phase at the output. Diffractive GPC provides amplitude and phase control at the input, which can be used for dynamic input optimization. As a common-path interferometer, GPC uses the low-frequency components of the phase modulation to create a reference wave for making the phase patterns visible. Hence, it would be problematic when the phase object does not have enough low-frequency components since the synthesized reference wave would then be too weak and so would generate interference patterns having poor contrast.

To illustrate the problem, we simulated the GPC output for a binary 0-π- checkerboard phase object. The resulting low-contrast output is shown in Fig. 3(A1). The light from the π-out-of-phase regions nearly canceled each other on-axis. This resulted in a very weak zero-order beam and synthesized reference wave that, in turn, resulted in a very low-contrast image. A perfectly symmetric phase pattern would not contain any zero-order component but, in this case, the truncation due to the circular aperture created an imbalance between the 0 and π regions, which left a residual reference wave and a poor-contrast output. We can improve the output contrast by extending the idea of diffractively-defined GPC apertures introduced in the previous section. In section 3, we used SLM-based grating regions to achieve amplitude modulation along a diffraction order and effectively created an adjustable circular aperture. We will now use diffractively defined apertures to not only create circular apertures but to spatially modulate the amplitude within these circular apertures as well.

To improve the GPC output, we will use the diffractive gratings at the input plane to apply spatial amplitude modulation onto the phase image. With the GPC system aligned along the proper diffraction order, we will effectively get an amplitude- and phase-modulated GPC input:

$$p_D(x,y) = a_D(x,y)\exp\left[\mathrm{i}\phi(x,y)\right], \tag{10}$$

#151449 - $15.00 USD Received 21 Jul 2011; revised 14 Sep 2011; accepted 3 Oct 2011; published 9 Jan 2012

which is essentially the same as the conventional input, Eq. (1), except that, this time, the amplitude modulation is not just a simple truncating aperture or the Gaussian profile of the laser beam, but can be arbitrarily chosen. Aside from this difference, the mathematical analysis is, otherwise, essentially equivalent to the conventional GPC.

To illustrate, let's consider the low contrast GPC output image shown in Fig. 3A1. Thresholding this image yields a binary checkerboard pattern, which we can use as basis for choosing the diffractive amplitude modulation pattern at the GPC input plane. Instead of using a 0-1 binary amplitude checkerboard pattern, we used a 0.5-1 input amplitude modulation pattern (see Fig. 3A3) so as to illuminate all the areas of the object. Implementing this amplitude modulation upsets the balance between the 0- and π-phase regions, which thereby strengthens the synthetic reference wave (SRW) and improves the contrast in the output image (see the improved contrast in Fig. 3 A2 and its linescan in Fig. 3A4; a linescan through the initial low-contrast image is included for comparison).

Figure 3B illustrates another application of diffractively modulated GPC in phase imaging. One issue in interferometric phase imaging is that different phases can have the same intensity in the resulting interference pattern. For example, $+\pi/2$ and $-\pi/2$ phase beams have the same intensity when interfering with a 0-phase reference beam. These phase ambiguities may be resolved in conventional interferometry by taking the interference pattern at different phase shifts of the reference beam [18]. We have previously used a similar approach in GPC by taking the GPC output for different phase shifts in the contrast filter [19]. This time, we will use a fixed phase-contrast filter and, instead, reconfigure the diffractive GPC input to resolve potential phase ambiguities in the GPC output.

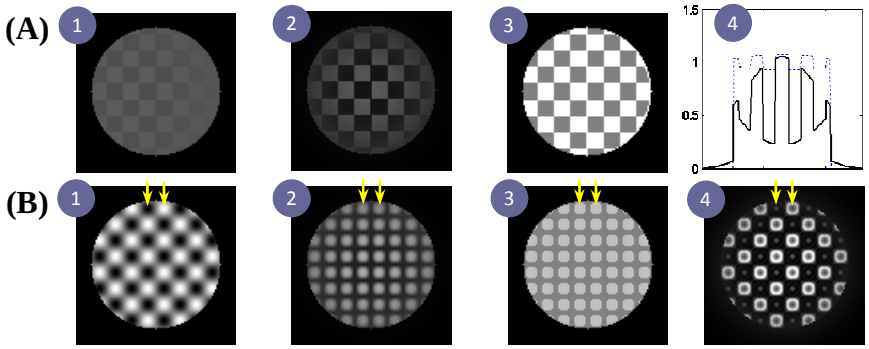

Fig. 3. Adaptive phase imaging using diffractively modulated GPC (simulations). (A) Contrast enhancement using adaptive spatial amplitude modulation: A GPC output with poor contrast, 1, is improved, 2, by using patterned illumination, 3, which is derived by thresholding the low-contrast image; 4 shows linescans through the center of images 1 (dotted) and 2 (solid). (B) Resolving phase ambiguity using adaptive spatial phase modulation: The arrows indicate that different phase values in a phase object, 1, can have degenerate intensities at the GPC output, 2, but superposing an additional phase modulation, 3, which is derived by thresholding the degenerate image can resolve these degeneracies at the output, 4.

Figure 3B 1 shows the grayscale representation of a phase object that we used in the simulations (white: $+\pi/2$; black:$-\pi/2$). Using this as the GPC input generates the output shown in Fig. 3B2. This output contains ambiguities since regions corresponding to positive and negative phase values both have the same intensity (e.g. see the arrows in Fig. 3B1 and 3B2). We can use this output pattern as basis for finding another phase modulation pattern that can help reveal the ambiguities. For example, we can threshold the ambiguous output pattern to get the pattern in Fig. 3B3. In this case, the diffractive phase input for GPC will correspond to the multiplication of this threshold pattern with the high-frequency grating. Projecting the phase object onto this diffractive input and then aligning the GPC system along the proper diffraction order creates the output intensity pattern shown in Fig. 3B4. Here the positive- and negative-phase regions now appear with different intensity. Hence, the additional phase offset allowed us to distinguish the phase between initially intensity-

#151449 - $15.00 USD Received 21 Jul 2011; revised 14 Sep 2011; accepted 3 Oct 2011; published 9 Jan 2012

degenerate regions. This shows that we can we use the diffractive phase modulation to introduce further spatial phase modulation onto a phase object to resolve phase ambiguities in the GPC output.

5. Optical security with fringe-based GPC for phase cryptography

Optical security is another potential application of diffractively-modulated GPC. Diffractive security devices such as holograms use gratings to create visual effects. Grating parameters like pitch, modulation depth and blaze angle are usually considered, but the grating phase is typically ignored. Spatially modulating the phase of the microgratings used in these security devices and then using them as diffractive inputs for GPC can enhance security by using phase as a new "machine-readable" information channel for further authentication.

In this regard, the results presented in Fig. 2 already provide proof-of-principle demonstrations. We just need to realize that the phase-modulated, circular diffractive aperture that generates, say Fig. 2C, could represent a circular micrograting on a security hologram. We can spatially modify the micrograting phase according to a desired hidden pattern and then reveal this pattern by GPC using the single modulation geometry in Fig. 1B. To further boost security, we may implement phase encryption (see [20] for more details), where we first encrypt the pattern that we wish to hide (e.g. using an XOR encryption key). The micrograting phase on the security hologram is spatially modulated according to the encrypted pattern.

When using phase encryption in security holograms, the hidden information can be retrieved by using the dual modulation system in Fig. 1A as a phase decryption system. The encrypted-phase-containing hologram is used as a phase object and placed on one modulation plane. The decryption key, which is identical to the encryption key for XOR encryption, may be combined with a second grating at the GPC input. Figure 4A and B show results of proof-of-concept experiments, where we used an LCoS SLM (Holoeye HOE 1080) to mimic holographic microgratings that we spatially shifted according to the encrypted phase pattern. We used another SLM (Hamamatsu PAL SLM) to encode the key. Figure 4A1 shows the low-contrast GPC output when using a wrong key. Although not so obvious due to the low contrast, we can actually make out the edges of the hidden pattern (the letters 'G','P', and 'C') even when using a wrong decryption key. To solve this problem, we can pixelate the hidden pattern so as to match the pixilation of the key pattern. Upon doing this, the edges of the hidden pattern are no longer visible when using a wrong decryption key as shown in Fig. 4A2. When using the correct key, the hidden pixilated pattern is revealed as a high-contrast image at the GPC output (Fig. 4A3). Even with the correct key in place, the pattern is again lost when the GPC is deactivated by removing the phase contrast filter (see the output in Fig. 4A4). Furthermore, Fig. 4B illustrates that a given security hologram containing encrypted phase patterns may be "personalized" even after its fabrication. Using the same dual SLM setup, we showed that we can generate different output patterns (Fig. 4B2-4) while using the same hologram by changing only the decryption key. In all cases, a wrong key produces a low contrast image (Fig. 4B1).

Moving one step further, we replaced the LCoS with a fabricated a hologram master. Figure 4C1 shows a white light image of the hologram master, which uses microgratings to create the observed visual features like colors and grayscale. The hologram contains a featureless central region where the microgratings have been phase-shifted according to both encrypted and unencrypted phase patterns. Using a laser to illuminate the hologram and aligning a 4*f* imaging system along one of the diffracted orders from the central region, we were able to capture an image the central region, as shown in Fig. 4C2. Aligning a phase contrast filter at the Fourier plane of the 4*f* system creates a GPC system that generates the output shown in Fig. 4C3. The GPC output reveals the hidden phase pattern, 'DTU', near the top of the circle. The central part of the circle contains encrypted patterns that are not revealed without the proper key. Upon using the correct decryption key, the GPC system is able to reveal the hidden pattern as shown by the captured GPC output presented in Fig. 4C4.

#151449 - $15.00 USD Received 21 Jul 2011; revised 14 Sep 2011; accepted 3 Oct 2011; published 9 Jan 2012

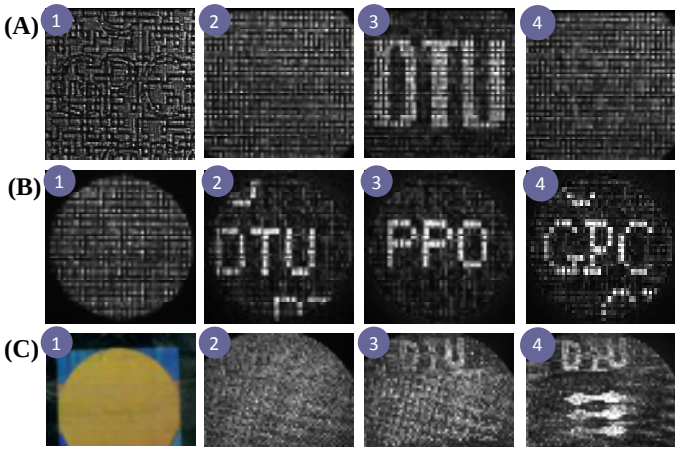

Fig. 4. Phase cryptography using diffractively modulated GPC. (A) Removing edge effects: The undecrypted output, 1, can show the edges of the hidden letters, but these are removed, **2**, by using pixilated letters, as seen in the decrypted GPC output pattern, **3**. This pattern disappears, **4**, when the GPC filter is removed; (**B**) Variable keys for an encrypted phase: the same encrypted phase, **1**, may contain different hidden patterns, **2**, **3**, **4**, that are only revealed by using the correct decryption keys. (**C**) Phase encryption using a hologram master: **1**, White light image of a master hologram with embedded phase within its featureless circular region; **2**, Image of laser diffraction from the circular region; **3**, Undecrypted GPC image of diffraction from the circular region; **4**, Final decrypted GPC image of the encrypted hologram master.

6. Conclusion and outlook

We introduced a new approach using Generalized Phase Contrast (GPC) having diffractively modulated inputs. We showed that this reproduces the results of conventional GPC, but with the new capacity to incorporate additional spatial amplitude and phase modulation to the GPC input. This new approach enables dynamic optimization for applications in patterned illumination and adaptive phase imaging. The available dynamic aperture control opens a new degree of freedom for improving phase imaging and we showed examples of how it can be done. Diffractively modulated GPC fits well with security micrograting and can exploit an added security layer by using the micrograting phase as an information channel, which can even be encrypted for adding yet another security layer.

Acknowledgments

We thank the Danish Technical Scientific Research Council (FTP) for financial support and Stensborg A/S for assistance with the hologram master fabrication.

#151449 - $15.00 USD Received 21 Jul 2011; revised 14 Sep 2011; accepted 3 Oct 2011; published 9 Jan 2012